JOURNAL OF ENGINEERING SCIENCES

Volume 11, Issue 2 (2024)

Aliyu S. A., Salahudeen N., Rasheed A. A. (2024). Adsorptive removal of lead (II) pollutants from wastewater using corncob-activated carbon. *Journal of Engineering Sciences (Ukraine), Vol. 11(2), pp. H1–H10.* https://doi.org/10.21272/jes.2024.11(2).h1

Adsorptive Removal of Lead (II) Pollutants from Wastewater Using Corncob-Activated Carbon

Aliyu S. A.[0009-0009-4033-6143], Salahudeen N.*[0000-0002-7537-8011], Rasheed A. A.

Department of Chemical and Petroleum Engineering, Bayero University, PMB 3011, Kano, Nigeria

Article info:
Submitted: April 3, 2024
Received in revised form: June 22, 2024
Accepted for publication: June 26, 2024
Available online: July 8, 2024

***Corresponding email:**
nsalahudeen.cpe@buk.edu.ng

Abstract: The level of contamination in industrial wastewater has been a serious environmental challenge of our time. Various researchers have reported that the adsorption process using different adsorbents is a promising technique for treating heavy metal-contaminated wastewater. This study investigated the adsorptive removal of lead (II) from wastewater using corncob-activated carbon. Activated carbon was synthesized from a raw corncob. The synthesized activated carbon was applied as a sorbent in batch lead (II) adsorption in an aqueous lead (II) solution. Scanning electron microscopy, Fourier transformed infrared (FTIR), and Brunauer–Emmett–Teller (BET) theory characterized the synthesized activated carbon. A batch adsorption study investigated the effects of dosage, contact time, and the initial concentration of lead (II) on the sorption of Pb^{2+} on the synthesized activated carbon. The highest removal of lead recorded was 95 % at an adsorbent dosage of 2.5 g/L in 2 h. The highest adsorption capacity was 16.46 mg/g at the same conditions. The results showed that percentage removal increased with dosage and contact time but decreased with the initial metal ion concentration. Adsorption kinetics were best described with the pseudo-second-order kinetics, while the Langmuir isotherm model best fitted equilibrium adsorption in the study. The FTIR results showed the presence of several functional groups like carboxyl, hydroxyl, and amino, indicating good interaction with lead metal ions. The BET characterization revealed the activated corncob's specific surface area and pore volume to be 249 m^2/g and 0.164 cm^3/g. This work shows that activated carbon can be synthesized from agricultural waste such as corncob and be used as an effective adsorbent for heavy metal removal, such as lead, from wastewater.

Keywords: metal-contaminated wastewater treatment, adsorption, corncob agro-waste, lead ion, adsorbent, isotherm, kinetics.

1 Introduction

Raw material mining and processing are key modern material development and value chain elements. Often and unintentionally, poisonous metallic impurities associated with mining and beneficiation processes are released into water streams as contaminants. The inevitability of material mining as a bedrock of industrialization has made heavy metal contamination in water streams a severe global problem. When employed on agricultural soil, heavy metal-contaminated water puts food safety in danger [1].

Heavy metals contaminated water releases poisonous anions possessing densities more than five times larger than that of water [2]. Unlike organic pollutants, which are most capable of biological degradation, heavy metals do not break down into benign byproducts [3]. The continuous growth of the human population has made the exponential increase in the need for portable water and the need to protect the environment from water pollutants a challenging global agenda [4]. Lead metal is one of the toxic metals that can be exposed to during industrial processes such as electroplating, paint manufacturing plants, textile manufacturing, steel, leather tanning, ceramic and glass industries, petroleum refining, battery manufacturing, mining operations, and other metal finishing industries [5].

Various techniques have been employed to eliminate excess heavy metals from aqueous solutions, including chemical precipitation, coagulation, flocculation, ion exchange, and reverse osmosis [6–10]. While these methods can be effective, their application is often

hindered by high operational costs, including the expense of chemicals, energy consumption, and equipment maintenance. In contrast, adsorption via biomass-based activated carbon has emerged as an attractive alternative due to its high efficiency in removing different pollutants [11]. This method converts biomass materials, usually regarded as wastes, into adsorbent to adsorb and remove heavy metals from solutions. Adsorption via activated carbon eliminates many disadvantages associated with conventional treatment methods by providing a more cost-effective and environmentally friendly option [10, 12–15].

Several natural and modified agricultural wastes and plants have been utilized to remove heavy metals in aqueous solutions. They include brewed tea waste, Palm kernel shells, chemically modified cashew nut shells, Africa elemi seed, mucuna and oyster shells, Azadirachta Indica leaves [1, 16, 17], Corncob [18, 19], and others. Corncobs are abundant agricultural wastes that can be effectively converted into activated carbon through carbonization and activation processes, presenting a promising avenue for improved adsorption efficiency. While there is significant research on the broader application of corncob-based adsorbents for heavy metal removal, the utilization of activated corncob specifically for lead removal appears to have received limited attention in the existing literature.

This study aimed to add value to corncob agricultural waste by converting it to activated carbon. The study's objective was to study the effectiveness of the synthesized activated carbon in the adsorptive removal of lead metal ions from aqueous solutions by determining the adsorptive removal efficiency, isotherms, and kinetics of lead sorption on corncob activated carbon.

2 Literature Review

Lead (II) can cause damage to the central nervous system, kidneys, liver, and reproductive systems [5]. Unregulated exposure to lead can slowly cause physical, skeletal, and neurological degenerative conditions such as sclerosis, Parkinson's disease, Alzheimer's disease, and muscular dystrophy [3]. Studies have shown that most heavy metals are mutagenic, carcinogenic, and teratogenic. Nearly every organ and system in the human body can be affected by lead, but children under the age of six are most vulnerable. [20]. The lead concentration in African, Asian, and European rivers and lakes was 83.8, 92.7, and 92.7 µg/L, respectively [16]. It was also reported that exposure at a concentration higher than (10 and 15 ng/L, according to the World Health Organization) can cause hepatitis, anemia, encephalopathy, and nephritic syndrome. Finding a sustainable method to remove heavy metals from water streams is crucial, especially in low- and middle-income nations that cannot afford to treat their water with expensive methods. Popular methods, such as electrochemical treatments, oxidation, filtration, and reverse osmosis, have been used to treat water previously contaminated with metal. However, these methods have been proven big-ticket [20].

Adsorption using inexpensive agricultural wastes is one alternate and promising technique that has recently attracted the attention of researchers [5]. Adsorption provides several advantages over traditional approaches, including low startup costs, convenience, flexibility, high selectivity, ease of use, environmental friendliness, insensibility to poisonous components, and its most significant potential for removing hazardous substances [16].

Activated charcoal is used as an adsorbent due to its remarkably high porosity, enhanced pore size, and higher adsorption capacities. However, due to high cost, its operation is somewhat inadequate [21]. Properties of activated carbon, such as surface functional groups, surface area, and pore size, can be modified to fit applications [22].

The adsorption process is influenced by several factors, such as adsorbent properties, pH, temperature, metal ion concentration, contact time, dosage, and competing ions [23–28]. Understanding these factors is crucial for optimizing adsorption processes and developing effective treatment strategies for pollutant removal in aqueous solutions.

Although there is extensive exploration into corncob-based adsorbents for heavy metal removal, studies such as [29–33] have provided a foundation for exploring the potential of corncob-based adsorbents for lead removal, in general, there is indeed a noticeable gap in detailed studies specifically in determining the efficiency, best isotherm model and kinetics of adsorption of lead ion over activated corncob adsorbent. Further research is needed to investigate activated corncob for lead removal to bridge the existing literature gap. Hence, these informed the fundamentals of the aim and objectives of this study, as outlined in the Introduction Section.

3 Research Methodology

3.1 Synthesis of activated carbon (AC) from corncob

The following chemical reagents were used in this study with highly purified analytical grades: Lead chloride (BDH Chemicals, Poole, England), Sulfuric acid (LOBAL Chemie, India), Nitrogen gas (United Industrial Gases, Kano, Nigeria), Sodium hydroxide (LOBAL Chemie, India), and Hydrochloric acid (LOBAL Chemie, India), Corncob (CDA, BUK), Crusher (220-240V Cob crusher, China), Muffle furnace (Nabertherm LT 5/12, Germany), Scanning electron microscope (PHENOM ProX, ThermoFisher Scientific, USA), FTIR (Agilent Technologies, USA), BET (Quantachrome NOVA 22002, USA), 0.45µm filter (Whatman, Germany), Atomic absorption spectrometer AAS (Agilent Technologies 240 FS, USA), pH meter (ST2100-B, OHAUS, USA), Shaker (JOANLAB, OS-20, China), Oven (Genlab Ltd., England), and Mesh (Kelsons, India).

The method of synthesis of activated carbon in this study was done by adapting the reported procedures of Fan et al. [34] and Ernest et al. [18]. The corncob was collected from the Centre for Dryland Agriculture (CDA). The corncob was washed with distilled water to remove dirt and impurities and then dried over sunlight for 2 days. Further, the corncob was placed in a hot air oven (Genlab Ltd., England) at 100 °C for 24 h for further drying. The corncob was then ground and sieved using a sieve of 75–200 µm (Kelsons, India). The prepared raw corncob powder (RC) was impregnated with H_2SO_4 in an equal ratio (w/w).

The impregnated sample was put in a muffle furnace (Nabertherm LT 5/12, Germany) and heated at 600 °C for 1.5 h at a 10 ºC/min heating rate. The resulting activated carbon (AC) sample was removed from the muffle furnace and washed with distilled water until neutral pH was achieved and then followed by drying in an oven (Genlab Ltd., England) at 105 °C for 2 h.

Figure 1 shows the pictural schematics of the activated carbon synthesis.

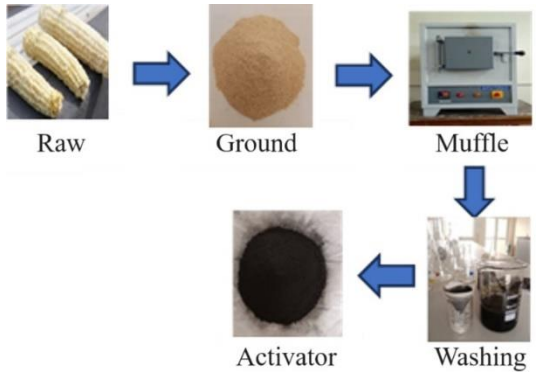

Figure 1 – Pictural schematics for the synthesis of activated carbon from corncob

3.2 Batch adsorption

Batch adsorption studies were conducted by adapting the methods of Ernest et al. [18], Chen et al. [19], and Batool et al. [35]. A stock solution of synthetic wastewater was produced by preparing 100 mg/l of lead (II) chloride salt in distilled water.

For each batch adsorption process, a specific amount of the synthesized adsorbent (AC) was added to a constant 80 ml of the 100 mg/l lead (II) chloride solution in 100 ml propylene bottles. The bottle was agitated on an orbital shaker (JOANLAB, OS-20 USA) at a constant speed of 150 rpm to study the effects of influential conditions on adsorption.

To investigate the effect of dosage, the adsorbent dosage was varied between 40–240 mg at intervals of 40 mg, and the batch adsorption was carried out at 150 rpm for 60 min at a constant concentration of 100 mg/l of the adsorbate. The optimum dosage obtained in the first instance was used to determine the effect of contact time varied from 20–140 min at 20 min while maintaining the same conditions.

Lastly, the effect of initial metal concentration was investigated by varying between 75–450 mg/l at intervals of 75 mg/l and using the optimum dosage and contact time obtained in the first two runs. Constant values of pH 7, 150 rpm, and room temperature were maintained throughout the studies. Each sample was withdrawn at the end of the batch adsorption process and filtered through a 0.45 µm filter paper. The filtrate residual lead (II) ion concentration was measured by atomic absorption spectrophotometer (Agilent Technologies 240 FS, USA). Equations (1) and (2) were used to analyze the adsorption data.

$$Q_e = \frac{V(C_i - C_e)}{M}; \quad (1)$$

$$PR = \frac{C_i - C_e}{C_i} \cdot 100\ \%, \quad (2)$$

where Q_e – the number of metal ions adsorbed at equilibrium, mg/g; PR – the percentage removal, %; C_i – the initial concentration of metal ions in solution, mg/L; C_e – the equilibrium concentration of metal ions in solution, mg/L; V – the volume of heavy metal solution, l; M – the mass of adsorbent, g.

The surface morphology of the activated carbon (AC) and that of the raw corncob (RC) were analyzed using a scanning electron microscope (PHENOM ProX, ThermoFisher Scientific, USA). The functional groups in the two samples were analyzed using Fourier transform infrared spectroscopy (Agilent Technologies, USA), and the specific surface area of the samples was determined using Brunauer-Emmett-Teller (Quantachrome NOVA 22002, USA).

3.3 Adsorption isotherm and kinetics

Three modes tested the kinetics of the lead (II) ion sorption process: Pseudo first order (PFO), Pseudo second order (PSO), and Intraparticle diffusion (IPD).

The following equations are the adsorption kinetics models for the PFO, PSO, and IPD:

$$Q_t = Q_e\left(1 - e^{-K_f t}\right); \quad (3)$$

$$Q_t = \frac{K_s Q_e^2 t}{1 + K_s Q_e t}; \quad (4)$$

$$Q_t = K_{id}\sqrt{t}, \quad (5)$$

where Q_e and Q_t – the adsorption capacity at equilibrium, mg/g; t – time, min; K_f – the rate constant of PFOA, min^{-1}; K_s – the rate constant of PSOA, g/(mg·min); K_{id} – the rate constant of IPD, mg/(g·$min^{0.5}$).

The adsorption isotherm was fitted by three different models: Langmuir isotherm (LI), Freundlich isotherm (FI), and Elovich isotherm (EI). The corresponding equations are as follows:

$$Q_e = \frac{bQ_m C_e}{1 + bC_e}; \quad (6)$$

$$Q_e = K_f C_e^{\frac{1}{n}}; \quad (7)$$

$$\frac{Q_e}{Q_m} = K_e C_e \, exp\left(-\frac{Q_e}{Q_m}\right), \quad (8)$$

where b and Q_m – Langmuir parameters related to maximum adsorption capacity and free energy of adsorption, respectively; K_f and n – Freundlich constants related to adsorption capacity and intensity of adsorption, respectively; K_e – an Elovich isotherm constant; C_e – the equilibrium concentration in the aqueous solution; Q_e – the equilibrium adsorption capacity of the adsorbent.

4 Results

The main results are presented in Figures 2–13 and Tables 1–3. Particularly, the effect of sorbent dosage on the percentage removal of lead ions is presented in Figure 2. The effect of initial metal ion concentration on percentage removal is presented in Figure 3.

The effect of contact time on percentage removal and adsorption capacity is presented in Figure 4. Also, figures 5–7 present the pseudo-2nd-order, pseudo-1st-order, and intraparticle diffusion adsorption kinetics, respectively.

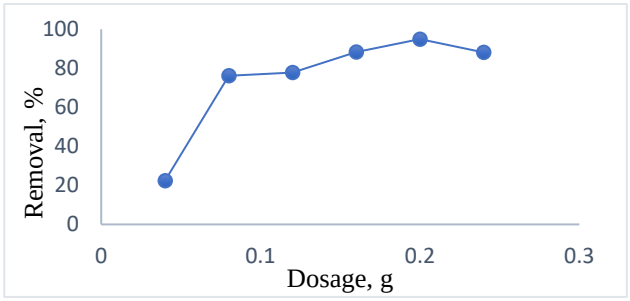

Figure 2 – Effect of sorbent dosage on percentage removal of sorbate

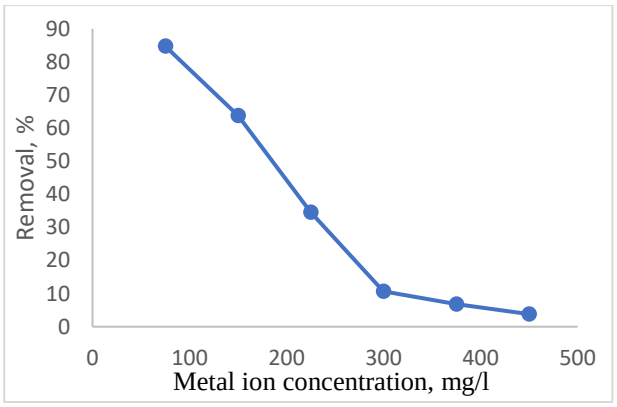

Figure 3 – Effect of initial metal ion concentration on percentage removal

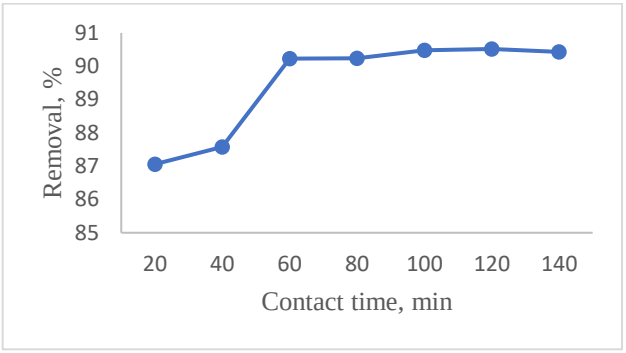

Figure 4 – Effect of contact time on percentage removal and adsorption capacity

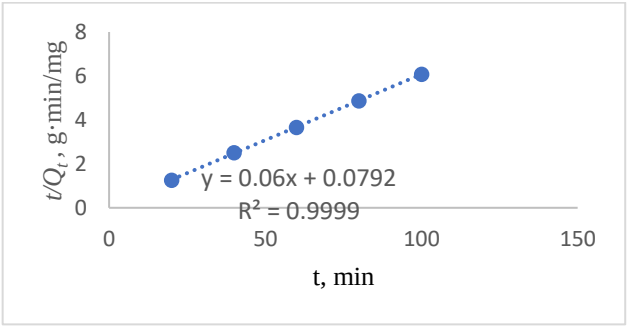

Figure 5 – Linearized plot of PSO

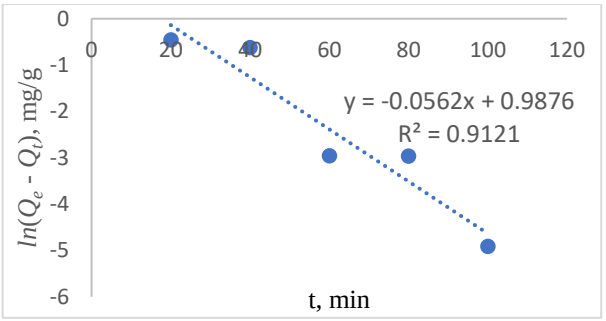

Figure 6 – Linearized plot of PFO

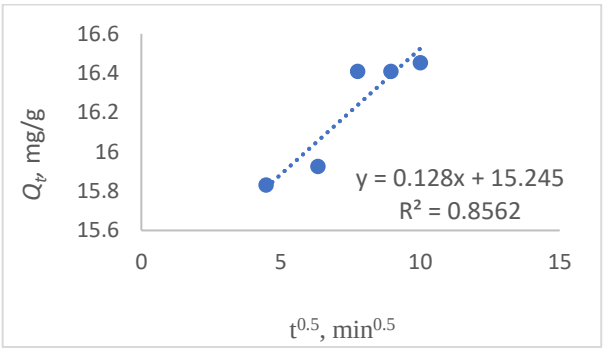

Figure 7 – Linearized plot of intraparticle diffusion

Tables 1 and 2 show the determined kinetic and isotherm parameters, respectively, indicating the regression correlation coefficient R^2.

Table 1 – Calculated values for different kinetic models

Model	Linearized equation	Parameters for the adsorption of lead (II) on AC
Pseudo-1st-order	$ln(Q_m - Q_t) = = lnQ_e - K_t$	Q_m = 9.72 mg/g; K_1 = 0.06 min^{-1}; R^2 = 0.912
Pseudo-2nd-order	$\frac{t}{Q_t} = \frac{1}{K_2 Q_e^2} + \frac{t}{Q_e}$	Q_e = 16.66 mg/g; K_2 = 0.76 g/(mg·min); R^2 = 0.999
Intraparticle diffusion	$Q_t = K_d\sqrt{t} + C$	K_{id} = 0.12 mg/(g·min$^{0.5}$); C = 15.24 mg/g R^2 = 0.856

Table 2 – Calculated values for different isotherm models

Model	Linearized equation	Parameters for the adsorption of lead (II) on AC
Langmuir	$\frac{C_e}{Q_e} = \frac{1}{Q_m K_L} + \frac{C_e}{Q_m}$	Q_m = 87.00 mg/g K_L = 0.04 mg/l R^2 = 0.954
Freundlich	$lnQ_e = lnK_f + \frac{1}{n} lnC_e$	K_f = 17.25 l/g n = 3.50 R^2 = 0.949
Elovich	$ln\frac{Q_e}{C_e} = lnK_e Q_m - \frac{Q_e}{Q_m}$	Q_m = 22.32 mg/g K_e = 1.12 R^2 = 0.872

Figures 8–10 present the Langmuir, Freundlich and Elovich isotherms, respectively. Figure 11 presents the SEM micrograph of the raw corncob and the synthesized activated carbon, respectively.

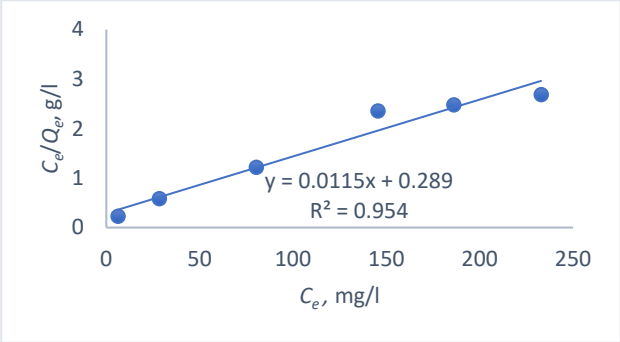

Figure 8 – Linearized Langmuir plot

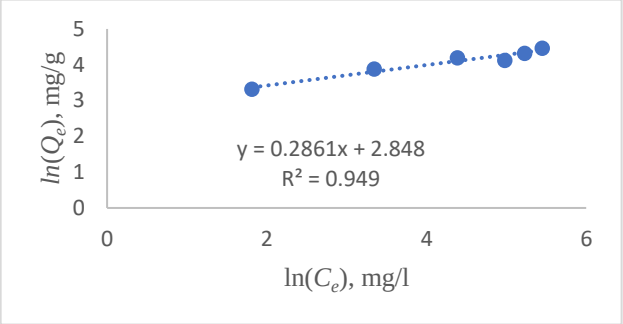

Figure 9 – Linearized Freundlich plot

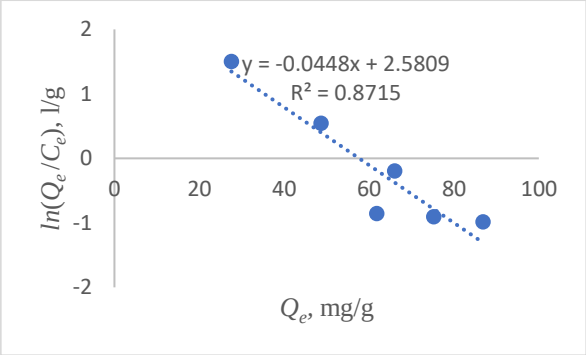

Figure 10 – Linearized Elovich plot

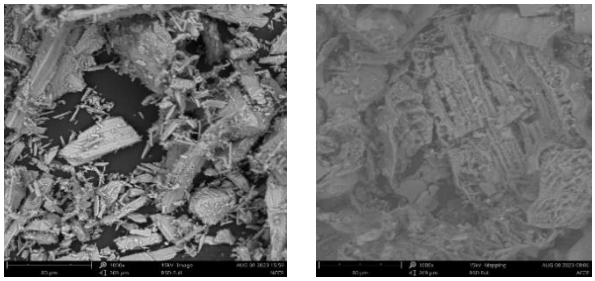

a b

Figure 11 – SEM micrograph for raw corncob (a) and synthesized activated carbon (b)

Table 3 shows the BET parameters of the raw corncob and the activated carbon synthesized.

Table 3 – BET results for raw corncob and activated carbon synthesized

Properties	RC	AC
BET surface area, m^2/g	104.4	249.0
BJH pore volume, cc/g	0.0648	0.1638
BHJ pore diameter, nm	2.144	1.853

Figures 12–13 present the FTIR of raw corncob and the synthesized activated carbon, respectively.

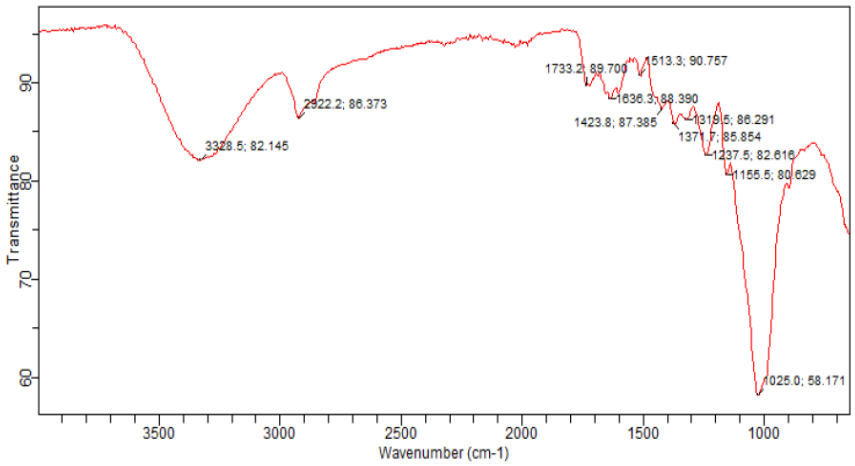

Figure 12 – FTIR of raw corncob (RC)

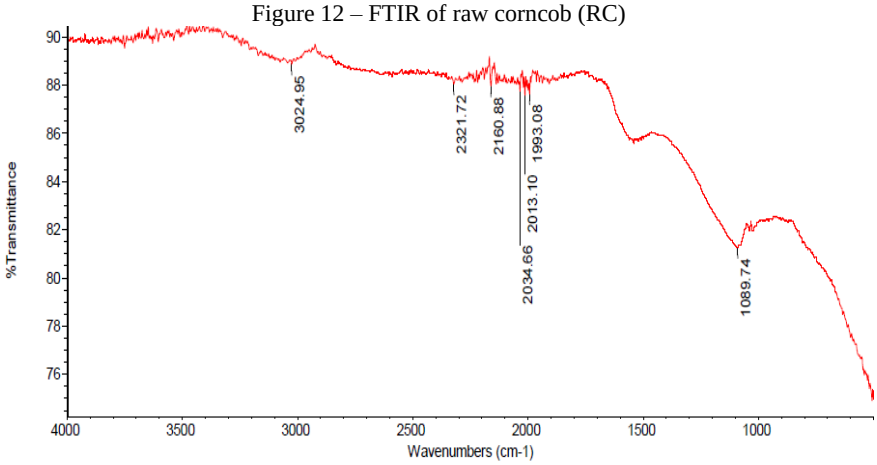

Figure 13 – FTIR of activated carbon (AC)

A microstructure was observed at ×1000 magnification, and an image of the sorbent was taken with a particle size of 269 µm.

Many steps, kinks, and broken edges can be observed on the external surface, which are likely to play an important role as active sites for adsorption.

5 Discussion

Figure 2 shows the effect of AC dosage against the percentage adsorption of the sorbent. Starting with 40 mg AC, the sorbate removal obtained was 22.3 %. When the dosage was doubled, the sorbent adsorption was more than triple, having sorbent adsorption of 76.1 % at an adsorbent dosage of 80 mg.

Further increases in the sorbent adsorption were observed at higher adsorbent dosage. At an adsorbent dosage of 160 mg, the corresponding sorbent adsorption was 88.3 %. However, only a marginal increment of sorbent adsorption was served at a further adsorbent dosage of 200 mg. The corresponding sorbent adsorption at 200 mg adsorbent dosage was 95 %. A further increase in the adsorbent dosage resulted in a reduction in the corresponding sorbent adsorption. This suggested that the optimum adsorption sites of the AC were available for binding the adsorbate molecules to the adsorption surface at 200 mg/(80 ml) adsorbent-to-adsorbate [1, 4].

Therefore, a further increase in the adsorbent dosage would not translate to increased sorbent adsorption at constant metal ion concentration [36].

Beyond the optimum adsorption dosage, a further increase will result in overlapping of the pores, thereby reducing the hindering efficiency of the adsorption process [37].

Figure 3 reveals that the threshold adsorption attained was 75 mg/l with almost 90 % removal. Meanwhile, it progressively decreased with an increase in metal concentration. This result may be explained by the fact that the available active sites are masked and saturated as the concentration increases, thus decreasing the removal percentage [16, 38].

However, the opposite trend for adsorption capacity was noticed for Pb (II) ions. Adsorption capacity increased with the initial concentration of the solution increasing. Greater uptake was recorded in solutions with higher initial concentrations [1, 39, 40]. At a lower initial concentration of metal ion and fixed adsorbent dosage, more vacant active sites are available, and thus, increasing the concentration will increase the adsorption capacity until saturation.

Figure 4 illustrates the effect of contact time on the percentage extent of removal and adsorption capacity. It can be seen that the percentage extent of removal increased smoothly in the first 40 min before it significantly hyped to over 90 % in 60 min. However, an unusual pattern was seen when the percentage removal decreased after 60 minutes and slightly increased by almost 0.3 % after 2 h. Therefore, the optimum contact time was attained in 2 hours with an extent of removal of 90.5 % and the adsorption capacity of 16.46 mg/g.

The findings are consistent with [37], which reported a similar optimum time of 2 h for lead (II) adsorption. That is to say, further prolonging the system had no remarkable effect on removing the metal ion [4, 16]. Overall, with an increment in intimate contact time of the adsorbent and the adsorbate, the rate of chemisorption increases sharply at first, then rises to the steady platform of negligible influence, and the instantaneous adsorption rate decreases gradually [40].

Figures 5–7 show the linear plots of the tested models. The results of the correlational analysis are presented in Table 1 with evaluated modes parameters. This study tested kinetic models, pseudo-1st-order, pseudo-2nd-order, and intraparticle diffusion models to reveal which best depicts the AC sorption of lead metal.

From Table 1, the pseudo-2nd-order (PSO) model had the highest value of the regression correlation coefficient $R^2 = 0.999$ and the evaluated theoretical adsorption capacity $Q_m = 16.66$ mg/g. These are the highest values of all the models fitted.

The main finding also agrees with studies [18, 41]. However, Yan et al. [2] reported that the lead and corn stover system can be described by PFO having higher R^2 than PSO. The kinetics data complied with PSO, indicating the predominant process was chemisorption [42].

Three isotherm models (Langmuir, Freundlich, and Elovich) were fitted to reveal the nature of the adsorption system between lead metal and activated carbon derived from Corncob. Figures (8) – (10) show the plots of the linearized forms of the mathematical equations where isotherm constants and correlation coefficient (R^2) of each model were calculated. Langmuir correlation coefficient and calculated adsorption capacity were the highest. Therefore, corncob-derived activated carbon's lead sorption system follows the Langmuir model and suggested monolayer adsorption [16, 17].

The presented study reveals that the Langmuir isotherm model can describe the adsorption of lead ions by activated Corncob. This agrees with the work of Yan et al. [2] and Chen et al. [19]. The highest monolayer adsorption capacity recorded for the adsorbent (AC) was 87.0 mg/g (Table 2).

From Figure 11b, the fiber bundles can be seen from the SEM of the RC; the structure and the morphology of the RC entirely changed when treated with sulfuric acid and heat. The fiber bundles in the RC were destroyed as a result of the decarbonization effect of the sulfuric acid on the fiber of the RC, thereby resulting in well-developed pores and the presence of more hydroxyl groups (OH^-) in the acidified RC. The increased availability of pores and OH^- group in the adsorbent makes it more effective for adsorption processes [41].

The presented study is in agreement with some past similar work [19, 43] where activated carbon was produced from corn stover with well-developed pores, and it looks like an eggshell structure with so many pores inside, like a honeycomb. A more rigid, tubular, and pore-like structure was observed in an activated carbon produced by [18], which concurs with the obtained result.

Table 3 presents the synthesized absorbent's specific surface area (SBET). The raw Corncob had a specific surface area of 104.4 m^2/g. This increased exponentially by 139 % to 249.0 m^2/g for the activated Corncob. Activated carbon almost tripled, and this trend is connected to the modification processes and conditions.

The surface area and the pore volume significantly increased after activation, and more pores were developed, thus making it a suitable adsorbent [22].

In the work of Yan et al. [2] and Chen et al. [19], it was observed that the S_{BET} of the acid/base-modified biochar was more significant than that of the unmodified Corncob. Aside from this, the essence of the modification is to enhance its adsorptive properties. However, Venkatrao and Sekhara [44] reported that the SBET of activated Corncob was more significant than obtained in the study.

The differences in the process conditions and the impregnating agents used for the two studies may be responsible for the difference. The AC yield is almost reduced to half. This phenomenon can be best described by the volatilization of lighter compounds and thermal degradation of lignocellulosic materials, and thus, it eventually leads to a lower yield of modified Corncob [45].

However, yield is a function of several optimum experimental conditions. Slow pyrolysis conducted by Borghol et al. [43] reported a yield of corn stover of 34 %, which is lower than expected when investigated at lower temperatures. Therefore, to optimize yield and efficient adsorbent, the influential parameters need to be optimized; hence, the materials are not the same in composition.

The Fourier transform infrared spectrum of the RC and the AC are shown in Figures (12) and (13), respectively. The FTIR bands observed in the RC spectrum at a wavenumber of $3.3 \cdot 10^3$ cm^{-1} was due to stretching hydroxyl groups (–OH) [46].

The band observed at $2.9 \cdot 10^3$ cm^{-1} was attributed to stretching (C–H) saturated functional groups [47]. The band observed at 1733.2 cm^{-1} was due to aldehyde (C=O), saturated aliphatic stretching [48].

The peak at $1.0 \cdot 10^3$ cm^{-1} was the prominent fingerprint attributed to (C-N) aliphatic amines.

Comparing the figures between RC and AC, it can be observed that some peaks shifted, disappeared, and new peaks were detected, which may be a result of the activation process. For instance, the FTIR bands observed in the RC at $3.3^{o}10^{3}$ cm^{-1} have disappeared in the AC spectrum. A new peak was now detected at a wavenumber of $3.0 \cdot 10^{3}$ cm^{-1}, which can be attributed to the vibrations of double bond compounds (=C-H) alkenes or (C-H) aromatics.

A band at $1.9 \cdot 10^{3}$ cm^{-1} was detected in the AC due to the vibrations of (C-N) aliphatic amines. It was observed that the band at $2.9 \cdot 10^{3}$ cm^{-1} was due to saturated hydrocarbons observed in the RC had been eliminated in the AC. This result agrees with [48].

The small band at $2.3 \cdot 10^{3}$ cm^{-1} for AC was attributed to (-C≡C-) acetylenes due to the dehydration reaction when sulfuric acid was added to the corncob. These results, therefore, suggest that corncob contains lipids, proteins, and carbohydrates. These functional groups can bind heavy metals through weak electrostatic interactions with ionic and Van der Waals forces [49].

6 Conclusions

Activated carbon synthesized from corncob was applied as an adsorbent to remove lead (II) contaminant from wastewater. The effect of dosage, contact time, and metal ion concentration on the removal efficiency was studied. The highest removal of lead observed was 95 % at an adsorbent dosage of 2.5 g/l for 2 h. The highest adsorption capacity recorded was 16.46 mg/g at the same conditions.

The results showed that the percentage removal generally increased with dosage and contract time but decreased with metal ion concentration. Adsorption kinetics were best fitted with the pseudo-2nd-order kinetics. The Langmuir isotherm model best fitted the equilibrium adsorption of lead in the study. The FT-IR results showed the presence of several functional groups (carboxyl, hydroxyl, and amino) which can interact with lead metal ions.

The BET characterization showed the activated corncob's specific surface area and pore volume to be 249 m^2/g and 0.164 cm^3/g, respectively. This study has shown that high adsorption efficiency activated carbon could be synthesized effectively from corncob agro-waste.

The synthesized corncob-activated carbon was effective for heavy metal removal, such as lead up to 95 % lead ion removal. The study further showed that the predominant adsorption mechanism was chemisorption, and a monolayer adsorption mechanism proceeded by the pseudo-2nd-order kinetics.

As a recommendation for further research opportunities, the techno-economic analysis of the conversion of agro-waste into activated carbon and the techno-economic analysis of the application for general treatment of industrial wastewater could be carried out. Furthermore, the efficiency and adsorption kinetics of treatment of the as-synthesized activated carbon with different sets of heavy metals other than lead could be studied.

Acknowledgments

The authors are grateful to the Tertiary Education Trust Fund, Abuja, for funding this project through their Institutional Base Research (IBR) grant No. BUK/DRIP/TETF/0012.

References

1. Baby, R., Saifullah, B., Hussein, M.Z. (2019). Palm kernel shell as an effective adsorbent for the treatment of heavy metal contaminated water. *Scientific Reports*, Vol. 9(1), 18955. https://doi.org/10.1038/s41598-019-55099-6
2. Yan, S., Yu, W., Yang, T., Li, Q., Guo, J. (2022). The adsorption of corn stalk biochar for Pb and Cd: Preparation, characterization, and batch adsorption study. *Separations*, Vol. 9(2), pp. 1–13. https://doi.org/10.3390/separations9020022
3. Garg, R., Garg, R., Sillanpää, M., Alimuddin, A., Khan, M.A., Mubarak, N.M., Tan, Y.H. (2023). Rapid adsorptive removal of chromium from wastewater using walnut-derived biosorbents. *Scientific Reports*, Vol. 13(1), 6859. https://doi.org/10.1038/s41598-023-33843-3
4. Gupta, V.K., Nayak, A., Bhushan, B., Agarwal, S.A (2015). Critical analysis on the efficiency of activated carbons from low-cost precursors for heavy metals remediation. *Critical Reviews in Environmental Science and Technology*, Vol. 45(6), pp. 613–668. https://doi.org/10.1080/10643389.2013.876526
5. Ali, I.H., Al Mesfer, M.K., Khan, M.I., Danish, M., Alghamdi, M.M. (2019). Exploring adsorption process of lead (II) and chromium (VI) ions from aqueous solutions on acid activated carbon prepared from Juniperus Procera leaves. *Processes*, Vol. 7(1), pp. 217–231. https://doi.org/10.3390/pr7040217
6. Abbas, G., Murtaza, B., Bibi, I., Shahid, M., Niazi, N.K., Khan, M.I., Amjad, M., Hussain, M, Natasha, N. (2018). Arsenic uptake, toxicity, detoxification, and speciation in plants: physiological, biochemical, and molecular aspects. *International Journal of Environmental Research and Public Health*, Vol. 15(1), 59. https://doi.org/10.3390/ijerph15010059
7. Altıntıg, E., Yenigun, M., Sarı, A., Altundag, H., Tuzen, M., Saleh, T.A. (2021). Facile synthesis of zinc oxide nanoparticles loaded activated carbon as an eco-friendly adsorbent for ultra-removal of malachite green from water. *Environmental Technology and Innovation*, Vol. 21, 101305. https://doi.org/10.1016/j.eti.2020.101305
8. Badmus, S.O., Oyehan, T.A., Saleh, T.A. (2021). Synthesis of a novel polymer-assisted AlNiMn nanomaterial for efficient removal of sulfate ions from contaminated water. *Journal of Polymers and the Environment*, Vol. 29, pp. 2840–2854. https://doi.org/10.1007/s10924-021-02077-7

9. Saleh, T.A. (2021). Protocols for synthesis of nanomaterials, polymers, and green materials as adsorbents for water treatment technologies. *Environmental Technology and Innovation*, Vol. 24, 101821. https://doi.org/10.1016/j.eti.2021.101821
10. Yılmaz, O., Tugrul, N. (2022). Zinc adsorption from aqueous solution using lemon, orange, watermelon, melon, pineapple, and banana rinds. *Water Practice and Technology*, Vol. 17(1), pp. 318–328. https://doi.org/10.2166/wpt.2021.102
11. Agrafioti, E., Bouras, G., Kalderis, D., Diamadopoulos, E. (2013). Biochar production by sewage sludge pyrolysis. *Journal of Analytical and Applied Pyrolysis*, Vol. 101, pp. 72–78. https://doi.org/10.1016/j.jaap.2013.02.010
12. Oyewole, O.A., Zobeashia, S.S.L.T., Oladoja, E.O., Raji, R.O., Odiniya, E.E., Musa, A.M. (2019). Biosorption of heavy metal polluted soil using bacteria and fungi isolated from soil. *SN Applied Sciences*, Vol. 1, 857. https://doi.org/10.1007/s42452-019-0879-4
13. Zhang, Y., Zheng, R., Zhao, J., Zhang, Y., Wong, P.K., Ma, F. (2013). Biosorption of zinc from aqueous solution using chemically treated rice husk. *BioMed Research International*, Vol. 2013, 365163. https://doi.org/10.1155/2013/365163
14. Karić, N., Maia, A.S., Teodorović, A., Atanasova, N., Langergraber, G., Crini, G., Ribeiro, A.R., Đolić, M. (2022). Bio-waste valorisation: Agricultural wastes as biosorbents for removal of (in) organic pollutants in wastewater treatment. *Chemical Engineering Journal Advances*, Vol. 9, 100239. https://doi.org/10.1016/j.ceja.2021.100239
15. Lutfee, T., Al-Najar, J.A., Abdulla, F.M. (2020). Removal of oil from produced water using biosorbent. *IOP Conference Series: Materials Science and Engineering*, Vol. 737(1), 012198. https://doi.org/10.1088/1757-899X/737/1/012198
16 Çelebi, H., Gök, G., Gök, O. (2020). Adsorption capability of brewed tea waste in waters containing toxic lead(II), cadmium (II), nickel (II), and zinc(II) heavy metal ions. *Scientific Reports*, Vol. 10(1), 17570. https://doi.org/10.1038/s41598-020-74553-4
17. Nuithitikul, K., Phromrak, R., Saengngoen, W. (2020). Utilization of chemically treated cashew-nut shell as potential adsorbent for removal of Pb(II) ions from aqueous solution. *Scientific Reports*, Vol. 10, 3343. https://doi.org/10.1038/s41598-020-60161-9
18. Ernest, E., Onyeka, O., Nkechi, O.J. (2019). Adsorption efficiency of activated carbon produced from corncob for the removal of cadmium ions from aqueous solution. *Academic Journal of Chemistry*, Vol. 4(4), pp. 12–20. https://doi.org/10.32861/ajc.44.12.20
19. Chen, F., Sun, Y., Liang, C., Yang, T., Mi, S., Dai, Y., Yu, M., Yao, Q. (2022). Adsorption characteristics and mechanisms of Cd^{2+} from aqueous solution by biochar derived from corn stover. *Scientific Reports*, Vol. 12, 17714. https://doi.org/10.1038/s41598-022-22714-y
20. Ismail, U.M., Onaizi, S.A., Vohra, M.S. (2023). Aqueous Pb(II) removal using ZIF-60: Adsorption studies, response surface methodology and machine learning predictions. *Nanomaterials*, Vol. 13(8), pp. 1402–1421. https://doi.org/10.3390/nano13081402
21. Patel, H. (2020). Batch and continuous fixed bed adsorption of heavy metals removal using activated charcoal from neem (Azadirachta Indica) leaf powder. *Scientific Reports*, Vol. 10(1), 16895. https://doi.org/10.1038/s41598-020-72583-6
22. Gale, M., Nguyen, T., Moreno, M., Gilliard-Abdulaziz, K.L. (2021). Physiochemical properties of biochar and activated carbon from biomass residue: Influence of process conditions to adsorbent properties. *ACS Omega*, Vol. 6(15), pp. 10224–10233. https://doi.org/10.1021/acsomega.1c00530
23. Foo, K.Y., Hameed, B.H. (2009). Utilization of biosorbents for the removal of hazardous dyes: A review. *Journal of Environmental Management*, Vol. 90(8), pp. 2313–2342. https://doi.org/10.1016/j.jenvman.2008.11.017
24. Park, H.-J., Na, C.-K. (2009). Adsorption characteristics of anionic nutrients onto the PP-g-AA-Am non-woven fabric prepared by photoinduced graft and subsequent chemical modification. *Journal of Hazardous Materials*, Vol. 166(2–3), pp. 1272–1278. https://doi.org/10.1016/j.jhazmat.2008.12.031
25. Crini, G. (2006). Non-conventional low-cost adsorbents for dye removal: a review. *Bioresource Technology*, Vol. 97(9), pp. 1061–1085. https://doi.org/10.1016/j.biortech.2005.05.001
26. Wang, S., Peng, Y. (2010). Natural zeolites as effective adsorbents in water and wastewater treatment. *Chemical Engineering Journal*, Vol. 156(1), pp. 11–24. https://doi.org/10.1016/j.cej.2009.10.029
27. Ho, Y.S., McKay, G. (1998). A comparison of chemisorption kinetic models applied to pollutant removal on various sorbents. *Process Safety and Environmental Protection*, Vol. 76(4), pp. 332–340. https://doi.org/10.1205/095758298529696
28. Kannan, N., Sundaram, M.M. (2001). Kinetics and mechanism of removal of methylene blue by adsorption on various carbons – A comparative study. *Dyes and Pigments*, Vol. 51(1), pp. 25–40. https://doi.org/10.1016/S0143-7208(01)00056-0
29. Nadeem, M., Ahmad, M., Nadeem, R. (2018). Review on heavy metals (Pb, Cu, Cd, Zn, Ni, Fe, Mn, Cr, and As) uptake by plants through phytoremediation. *International Journal of Environmental Research and Public Health*, Vol. 15(1), 59. https://doi.org/10.3390/ijerph15010059
30. Rongwong, W., Goh, K. (2020). Resource recovery from industrial wastewaters by hydrophobic membrane contactors: A review. *Journal of Environmental Chemical Engineering*, Vol. 8(5), 104242. https://doi.org/10.1016/j.jece.2020.104242
31. Du, S., Cao, Y., Fang, G., Qiao, S. (2021). Activated carbon derived from corn cob for efficient removal of heavy metals from wastewater: A review. *Bioresource Technology Reports*, Vol. 14, 100668. https://doi.org/10.1016/j.biteb.2020.100668
32. Ncibi, M.C., Mahjoub, B., Seffen, M., Hamza, M.F., Mlayah, A., Aloui, F. (2021). Activated carbon prepared from corn cob as an efficient adsorbent for the removal of heavy metals: A review. *Journal of Environmental Management*, Vol. 287, 112291. https://doi.org/10.1016/j.jenvman.2021.112291
33. Zhu, W., Zhang, X., Ma, Y., Guan, J. (2021). Recent advances in flocculation technology for heavy metal removal: A critical review. *Chemical Engineering Journal*, Vol. 427, 131690. https://doi.org/10.1016/j.cej.2021.131690
34. Fan, S., Sun, Y., Yang, T., Chen, Y., Yan, B., Li, R., Chen, G. (2020). Biochar derived from corn stalk and polyethylene co-pyrolysis: Characterization and Pb(II) removal potential. *RSC Advances*, Vol. 10(11), pp. 6362–6376. https://doi.org/10.1039/c9ra09487c
35. Batool, F., Akbar, J., Iqbal, S., Noreen, S., Bukhari, S.N.A. (2028). Study of isothermal, kinetic, and thermodynamic parameters for adsorption of cadmium: An overview of linear and nonlinear approach and error analysis. *Bioinorganic Chemistry and Applications*, Vol. 2018, 3463724. https://doi.org/10.1155/2018/3463724
36. Brishti, R.S., Kundu, R., Habib, M.A., Ara, M.H. (2023). Adsorption of iron (III) from aqueous solution onto activated carbon of a natural source: Bombax ceiba fruit shell. *Results in Chemistry*, Vol. 5, 100727. https://doi.org/10.1016/j.rechem.2022.100727

37. Alghamdi, A.A., Al-Odayni, A.B., Saeed, W.S., Al-Kahtani, A., Alharthi, F.A., Aouak, T. (2019). Efficient adsorption of lead (II) from aqueous phase solutions using polypyrrole-based activated carbon. *Materials*, Vol. 12(12), 2020. https://doi.org/10.3390/ma12122020
38. Wu, C.H., Kuo, C.Y., Guan, S.S. (2016). Adsorption of heavy metals from aqueous solutions by waste coffee residues: Kinetics, equilibrium, and thermodynamics. *Desalination and Water Treatment*, Vol. 57(11), pp. 5056–5064. https://doi.org/10.1080/19443994.2014.1002009
39. Thabede, P.M., Shooto, N.D., Naidoo, E.B. (2020). Removal of methylene blue dye and lead ions from aqueous solution using activated carbon from black cumin seeds. *South African Journal of Chemical Engineering*, Vol. 33, pp. 39–50. https://doi.org/10.1016/j.sajce.2020.04.002
40. Wang, B., Lan, J., Bo, C., Gong, B.,Ou, J. (2023). Adsorption of heavy metal onto biomass-derived activated carbon: Review. *RSC Advances*, Vol. 13(7), pp. 4275–4302. https://doi.org/10.1039/d2ra07911a
41. Wang, Y., Li, S., Ma, L., Dong, S., Liu, L. (2020). Corn stalk as starting material to prepare a novel adsorbent via SET-LRP and its adsorption performance for Pb(II) and Cu(II). *Royal Society Open Science*, Vol. 7(3), 191811. https://doi.org/10.1098/rsos.191811
42. Liu, L., Yang, W., Gu, D., Zhao, X., Pan, Q. (2019). In situ preparation of Chitosan/ZIF-8 composite beads for highly efficient removal of U(VI). *Frontiers in Chemistry*, Vol. 7(1), pp. 607–617. https://doi.org/10.3389/fchem.2019.00607
43. Borghol, J., El-Kady, M.Y., Khalil, M.H., El-Malky, M., Abd-Elatif, A.A. (2019). Using of date palm leaf midrib biochar as an adsorbant in water treatment. *Journal of Environmental Sciences*, Vol. 48(3), pp. 1-20. https://doi.org/10.21608/JES.2019.160146
44. Venkatrao, C., Sekhara, D.R. (2019). Preparation of Activated carbon from corncob for multiple adsorption of heavy metal ions in aqueous solution. *Journal of Emerging Technologies and Innovative Research*, Vol. 6(6), pp. 488–501.
45. Shakya, A., Vithanage, M., Agarwal, T. (2022). Influence of pyrolysis temperature on biochar properties and Cr (VI) adsorption from water with groundnut shell biochars: Mechanistic approach. *Environmental Research*, Vol. 215(1), 114243. https://doi.org/10.1016/j.envres.2022.114243
46. Chen, F., Sun, Y., Liang, C., Yang, T., Mi, S., Dai, Y., Yao, Q. (2022). Adsorption characteristics and mechanisms of Cd^{2+} from aqueous solution by biochar derived from corn stover. *Scientific Reports*, Vol. 12, 17714. https://doi.org/10.1038/s41598-022-22714-y
47. Yan, S., Yu, W., Yang, T., Li, Q., Guo, J. (2022). The adsorption of corn stalk biochar for Pb and Cd: Preparation, characterization, and batch adsorption study. *Separations*, Vol. 9(2), 22. https://doi.org/10.3390/separations9020022
48. Vilardi, G., Di Palma, L., Verdone, N. (2018). Heavy metals adsorption by banana peels micro-powder: Equilibrium modeling by non-linear models. *Chinese Journal of Chemical Engineering*, Vol. 26(3), pp. 455–464. https://doi.org/10.1016/j.cjche.2017.06.026
49. Khan, T.A., Mukhlif, A.A., Khan, E.A. (2017). Uptake of Cu^{2+} and Zn^{2+} from simulated wastewater using muskmelon peel biochar: Isotherm and kinetic studies. *Egyptian Journal of Basic and Applied Sciences*, Vol. 4(3), pp. 236–248. https://doi.org/10.1016/j.ejbas.2017.06.006